Generalized WKB and Milne solutions to one-dimensional wave equations

F. Robicheaux, U. Fano, and M. Cavagnero*
Department of Physics and The James Franck Institute, University of Chicago, Chicago, Illinois 60637

D. A. Harmin
Department of Physics and Astronomy, University of Kentucky, Lexington, Kentucky 40506
(Received 10 December 1986)

Diverse semianalytical constructions of wave functions, approximate or exact, are combined through the introduction of novel concepts. These include representing wave functions by a mosaic of analytic functions of a phase variable ϕ, each of them adapted to the problem's features over a restricted range of a coordinate x, and focusing the numerical effort on the metric relation between ϕ and x. This shift of attention from the wave function proper to metric relations is viewed as the essence of the Milne approach and of its WKB approximation. Illustrative examples are worked out and discussed.

I. INTRODUCTION

The initial Wentzel-Kramers-Brillouin (WKB) (Ref. 1) approximation for solving one-dimensional wave equations is simple and transparent but subject to notorious shortcomings. A number of variants have been introduced since the early days of wave mechanics to compensate these shortcomings[2–7]—e.g., by using Airy functions instead of sines—often with overlapping elements. Each variant appears to stem from a limited context, with scarce illustration by specific examples. One aim of this paper is to cast these variants in a single mold and to illustrate their operation.

A second and more novel aim is to stress and exploit the intimate connection between the WKB approximation and Milne's exact method of solving wave equations in terms of a sine function.[8,9] Judicious combination of existing procedures will afford a transparent and economic path to semianalytical representation of the exact solution, at least in the examples to be presented here.

Various extensions of the WKB method will be rederived in Sec. II by rescaling the independent and dependent variables of a wave equation. Scaling—a unifying feature of WKB and Milne approaches—replaces the space coordinate x by a suitably defined phase of oscillation $\phi(x)$ of an analytical function whose nodes lie, by definition, at specified values of its phase variable. Phase and amplitude functions are then related through the wave equation, often in the form of dispersion relations.

Section III will show how a Milne treatment of a wave equation selects at the outset an analytical representation of its solution and then proceeds to *calculate the metric* of the scaling transformation instead of calculating the wave function itself. This procedure affords inherent economy because the metric generally varies smoothly in space, in contrast to the oscillations of the wave function. A suitable ansatz may even represent the metric in terms of a few parameters. Guidelines for selecting sensible representations will stress the use of different analytical representations in different ranges of the space coordinate, as in the quantum-defect treatment of atomic wave functions.[10]

This paper amounts, in essence, to setting a policy for the better use of previously known analytical tools. [This policy has emerged in the course of implementing an adiabatic (i.e., WKB) approach to nonseparable multidimensional wave equations,[11] a subject of special interest to quantum chemistry.[12] The policy appears well suited for calculating Schrödinger eigenfunctions in two or more dimensions in terms of suitably curved phase coordinates, but its application remains to be developed fully.]

Here we deal with the one-dimensional wave equation

$$d^2y/dx^2+k^2(x)y(x)=0 \ . \tag{1}$$

The WKB approximation to $y(x)$ presupposes slow variation of $k^2(x)$ over distances of the order of the wavelength

$$\lambda\!\!\!^{-}=1/k(x) \ , \tag{2}$$

a condition represented by the equivalent relations[13]

$$\left|\frac{d\,|k^2|}{d(x/\lambda\!\!\!^{-})}\right| \ll k^2 \ , \quad \left|\frac{d\ln(k^2)}{dx}\right| \ll |k| \ , \quad d\lambda\!\!\!^{-}/dx \ll 1 \ . \tag{3}$$

When derivatives of $k(x)$ are disregarded altogether, the solution of (1) is represented by a trigonometric function

$$y(x)\propto \sin S(x) \ , \quad S(x)=\int^x k(x')dx' \ , \tag{4a}$$

for $k^2(x)>0$, and by

$$y(x)\propto \exp\pm\int^x |k(x')|\,dx' \tag{4b}$$

for $k^2(x)<0$. Integration constants omitted in (4) are determined by boundary or phase-matching conditions. The first-order correction to the solutions (4) yields the familiar expressions

$$y(x)=[k(x)]^{-1/2}\sin\int^x k(x')dx'+O(|d\lambda\!\!\!^{-}/dx|^2) \ , \tag{5a}$$

$$y(x)=|k(x)|^{-1/2}\exp[\pm\int^{x}|k(x')|dx'] +O(|d\lambda/dx|^{2}) . \quad (5b)$$

The factors $|k(x)|^{-1/2}$ in (5) normalize the function (4) to reflect a focusing effect of variations of $k^2(x)$, namely, the concentration of wave intensity where $k^2(x)$ is lower. (In wave mechanics a particle is found with higher probability where its speed is lower.) The solutions (5) clearly fail at "classical turning points" where $|k(x)|$ vanishes and their amplitude diverges. "Connection formulas" were introduced early in wave mechanics[2] to bridge the gap between ranges of x where (5a) or (5b) holds, respectively. Soon thereafter more general procedures were developed that bypass the difficulties generated by nodes or poles[4] of $k^2(x)$.

"Extended WKB" procedures, partially codified by Miller and Good,[5] replace the sine or exponential in (4) and (5) by alternative analytical functions which solve a model wave equation exactly. (Note that singular points of physical problems, such as the nodes and poles of $k^2(x)$, generally call for an analytic solution.) Sec. II will show how WKB procedures amount to mapping Eq. (1) onto analytically solvable models. Section III will then discuss how to bypass the WKB approximation altogether in the one-dimensional setting by shifting emphasis from direct construction of $y(x)$ to the more benign problem of constructing the metric of a phase coordinate. Section IV will present illustrations.

II. SCALING TRANSFORMATION AND WKB APPROXIMATION

We study here the transformation of the wave equation (1) induced by replacing the space coordinate x by a generic phase function $\phi(x)$ [which coincides with $S(x)$ of (4a) in a special case]. This transformation may be performed directly by differential procedures but emerges more coherently when (1) is viewed as the Euler equation of the variational integral[14]

$$\delta\int_{x_0}^{x_1}dx\left[\left[\frac{dy}{dx}\right]^2-k^2(x)y^2(x)\right]=0 , \quad y(x_0)=y(x_1)=0 . \quad (6)$$

The value and the structure of this integral remain invariant under the following set of joint transformations:

$$x\rightarrow\phi(x) , \quad dx=h(x)d\phi , \quad d\phi=h^{-1}dx , \quad (7)$$

$$y\rightarrow Y , \quad y=h^{1/2}Y , \quad Y=h^{-1/2}y , \quad (8)$$

$$k\rightarrow K , \quad k^2(x)=h^{-2}\left[K^2(\phi)-\frac{1}{2}\frac{d^2\ln h}{d\phi^2}+\left[\frac{1}{2}\frac{d\ln h}{d\phi}\right]^2\right] , \quad (9a)$$

$$K^2(\phi)=h^2\left[k^2(x)+\frac{1}{2}\frac{d^2\ln h}{dx^2}+\left[\frac{1}{2}\frac{d\ln h}{dx}\right]^2\right] , \quad (9b)$$

which yield

$$\delta\int_{\phi_0}^{\phi_1}d\phi\left[\left[\frac{dY}{d\phi}\right]^2-K^2(\phi)Y^2(\phi)\right]=0 , \quad Y(\phi_0)=Y(\phi_1)=0 . \quad (10)$$

The following stepping stones in the derivation of (8) are noted:

(a) The single transformation (7) changes (6) into

$$\delta\int_{\phi_0}^{\phi_1}d\phi\, h\left[\left[\frac{1}{h}\frac{dy}{d\phi}\right]^2-k^2y^2\right]=0 . \quad (11)$$

(b) The renormalization (8) serves to change the dimensions $[x]^{-2}$ of the squared wave number $k^2(x)$ to the dimensions $[\phi]^{-2}$ of h^2k^2.

(c) Derivatives of the metric function h,

$$dh/dx=h^{-1}dh/d\phi=d\ln h/d\phi , \quad (12)$$

appear when the expression (8) of y is entered in (11), yielding

$$\begin{aligned}\frac{1}{h}\left[\frac{dy}{d\phi}\right]^2&=\left[\frac{dY}{d\phi}+\frac{1}{2}\frac{d\ln h}{d\phi}Y\right]^2\\&=\left[\frac{dY}{d\phi}\right]^2+\frac{d\ln h}{d\phi}Y\frac{dY}{d\phi}+\left[\frac{1}{2}\frac{d\ln h}{d\phi}\right]^2Y^2\\&=\left[\frac{dY}{d\phi}\right]^2+\frac{1}{2}\frac{d}{d\phi}\left[\frac{d\ln h}{d\phi}Y^2\right]\\&\quad+\left[-\frac{1}{2}\frac{d^2\ln h}{d\phi^2}+\left[\frac{1}{2}\frac{d\ln h}{d\phi}\right]^2\right]Y^2 . \quad (13)\end{aligned}$$

The middle term of the last expression in (13)—a total derivative—does not contribute to the variational integral (10), thus eliminating from (10) any first derivative of Y. The derivatives of $\ln h$ in (13) are incorporated in (9a) and (9b).

The immediate result of the transformations (7)—(9) is to replace the wave equation (1)—the Euler equation of the variational expression (6)—with the wave equation pertaining to (10), namely,

$$d^2Y/d\phi+K^2(\phi)Y(\phi)=0 . \quad (14)$$

Our goal is to exploit the flexibility built into (14) by the latitude in selecting the phase function $\phi(x)$. Specific attention will center on the metric function $h=dx/d\phi$, rather than on $\phi(x)$ itself, and still more pointedly on the transformation formulas (9) that interconnect $k^2(x)$, $K^2(\phi)$ and the metric h. Since $k^2(x)$ is fixed by our initial equation (1), we should optimize the selection of $K^2(\phi)$ and $h(x)$ subject to the constraint of (9).

The logarithmic derivative terms of (9) are an important element of this constraint. Being of second order in the rate of variation of the metric h, they will be disregarded within the WKB approximation of this section, just as the second derivatives of $k^2(x)$ are disregarded in the traditional WKB treatment. The relations (9), however, suggest a more specific condition for their derivative terms to remain small, namely, that the $K^2(\phi)/k^2(x)$ vary

slowly. This condition will prove critical to the application of Milne's method in Sec. III.

A. Extended WKB approximation

The diverse earlier extensions of WKB (Refs. 3—7) are viewed here in terms of a single common element: We solve (14) analytically, with the constraint (9) on $\{K^2(\phi),h(x),k^2(x)\}$ shorn of its logarithmic derivatives, that is, cast in its approximate form of wave-number scaling,

$$K^2(\phi)\approx h^2(x)k^2(x)=\left[\frac{dx}{d\phi}k(x)\right]^2 . \tag{15}$$

Within this scope the original WKB solutions (5) amount to setting

$$\begin{aligned}&\phi(x)=S(x)=\int^x k(x')dx' ,\\ &h(x)=1/k(x) ,\\ &K^2(\phi)=1 .\end{aligned} \tag{16}$$

Replacing the constraint (9) by its abbreviated form (15) is viewed here as appropriate to a WKB approximation, in accordance with the earlier discussion. We shall hold to this approximation in the present Sec. II A and in the following Sec. II B, which discuss the solution of (14) under the constraint (15) for various examples of wave-number functions $k^2(x)$, that is, of refractive index or potential. The derivative terms of (9) will be considered again in Sec. II C and especially in Sec. III which exceed the scope of WKB approximations.

The intent as well as the actual construction of the mapping $\phi(x)$ emerge from the alternative form of (15),

$$h=\frac{dx}{d\phi}=\frac{K(\phi)}{k(x)} . \tag{17}$$

Insofar as the zeros and singularities of $k(x)$ are cancelled by corresponding features of $K(\phi)$ in their ratio (17), the metric function $h(x)$ subsumes the remaining smoothly varying features of $k(x)$. Our procedure should then ensure that the metric $h=dx/d\phi$ be real, smooth and amenable to easy numerical treatment, consistent with analytic solution of (14). The explicit construction of the mapping $\phi(x)$ is generally achieved through the integral form[5] of (17)

$$\int_{\phi_0}^{\phi}K(\phi')d\phi'=\int_{x_0}^{x}k(x')dx'=S(x) . \tag{18}$$

Setting the lower limits of integration (ϕ_0,x_0) amounts to selecting an integration constant that anchors the scale of ϕ to that of x. The functions K and k in (18) are often singular but the effects of their singularities cancel in the ratio (17).

Zeros of $k^2(x)$ at positions $x=x_i$ are removed from the metric ratio (17) by adopting the polynomial form of $K^2(\phi)$,

$$K^2(\phi)=\Pi_i[\phi(x)-\phi(x_i)] . \tag{19}$$

When a single zero occurs in a range of interest, (14) is solved by an Airy function, as detailed in Sec. IV A. A pair of zeros leads to parabolic cylinder functions (Sec. IV B), which may be represented as Coulomb field wave functions of ϕ^2. A pair of zeros *outside* the real axis may be usefully included in (19) to represent variations of $k^2(x)$ near a minimum or maximum,

$$k^2(x)\propto(x-\mathrm{Re}x_i)^2+(\mathrm{Im}x_i)^2 , \tag{20}$$

which are sharp for small values of $\mathrm{Im}x_i$. Three or four zeros lead to representing $Y(\phi)$ as a function of elliptic integrals, but may be handled more effectively by joining piecewise solutions in alternative regions, each region with one or two zeros only (see Sec. II B below).

The main singularities of $k^2(x)$ encountered in physical problems arise from centrifugal potentials,[15] with $k^2\propto(x-x_j)^{-2}$. These are treated by setting $K^2(\phi)=1+b/(\phi-\phi_j)^2$, whereby $Y(\phi)$ is a Bessel-type function (Sec. IV C). Coulomb field singularities, $k^2(x)\propto 1/x$, are instead removed by setting $\phi\propto\sqrt{x}$ (Sec. IV D).

B. Mosaics of locally adapted $Y(\phi)$

The task has been formulated of selecting a scaled wave-number function $K(\phi)$ that embodies salient features of the initial $k(x)$ and yet affords analytical solution of (14). The task is generally subject to the difficulty of building into a single $K(\phi)$ all the features of $k(x)$—nodes, poles, etc.—that occur in different ranges of x. To bypass this difficulty one may select two or more different analytical representations of $K(\phi)$, and hence different phase functions $\phi(x)$ and metrics h, to be utilized in different ranges of the independent variable x. The corresponding alternative representations of the solution $y(x)=\sqrt{h}\,Y(\phi)$ appropriate to the several ranges of x have then to be matched in amplitude and phase at each boundary between such ranges. This additional operation is often the price to be paid to secure a realistic representation of $y(x)$. This price is modest in terms of computing effort. On the other hand the transparency of WKB solutions represented by one or a few analytical functions $\sqrt{h}\,Y(\phi)$ would be nullified by using too many piecewise representations.

This essential aspect of extended WKB procedures, anticipated in Sec. I, does not seem to have been stressed adequately in the past even though it was clearly implied by the use of connection formulas that join (5a) with (5b). Of course, the construction of an eigenfunction $y(x)$ over an extended range of x as a mosaic of different "locally adapted" solutions does *not* hinge on the use of the WKB approximation, even though it is introduced here in a WKB context. In fact the mosaic procedure may well prove itself mainly in the broader context of Sec. III.

Comparing the WKB treatment of the wave equations for a particle confined to a single-or to a double-potential well illustrates the need to represent a wave function differently in different regions of space. On the one hand, the single-well problem lends itself to representation by a single parabola

$$K^2(\phi)=a-b\phi^2(x) , \quad (a,b)>0 \tag{21}$$

in which case $Y(\phi)$ is an oscillator wave function, i.e., one of the main types of parabolic cylinder functions. The

value $\phi=0$ corresponds here to the bottom of the well and $\phi=\pm(a/b)^{1/2}$ to the turning points of the classical motion. Any asymmetry of the well represented by the actual function $k^2(x)$ is then built into the metric function $h(x)=dx/d\phi$ and so is any lesser departure of $k^2(x)$ from a parabolic shape. Replacement of $k^2(x)$ by (20) and representation of the solution of (1) in terms of an oscillator function, $y(x)=\sqrt{h}\,Y(\phi)$, will prove adequate insofar as the resulting values of the last two terms of (9) are negligible.

The double-well potential, on the other hand, presents a more varied challenge, in that the barrier between the wells has generally a finite height and a profile quite different from the barriers on either side of the double well. Different types of analytical $K^2(\phi)$ are then required for a realistic representation of the two barriers, even though both may be locally parabolic. Correspondingly different types of parabolic cylinder functions $Y(\phi)$ are then appropriate to represent $y(x)$ in the central and outer parts of the double well. A single matching of such different representations of $y(x)$ will be sufficient if $k^2(x)$ is symmetric under reflection through the center of the double well. Otherwise $y(x)$ would need to be constructed as a mosaic of three or four sections. Generally *each* locally adapted analytic representation of $y(x)$ should embody the influence of *a major feature* of $K^2(x)$.

The procedure for matching the amplitude and slope of wave functions at the boundary $x=x_p$ of two sections, namely, $y_1(x)$ for $x\le x_p$ and $y_2(x)$ for $x\ge x_p$ is equivalent to that in use for joining segments of radial wave functions identified by initial conditions at $r=0$ and ∞, respectively.[16] Recall here that the construction of wave functions for a particle bound in a single or multiple well also involves the determination of an eigenvalue such as the one represented by the parameter a in (21). The standard matching procedure at a boundary $x=x_p$—or at a sequence of boundaries—reduces to a linear homogeneous system thereby determining the relevant eigenvalue. Examples of this procedure will be described in Sec. IV.

By determining the eigenvalue, the matching procedure also controls the occurrence of standing wave solutions, $y(x)$ or $Y(\phi)$, that meet the boundary conditions at both ends of the full range of x. The traditional WKB procedure met the same goal speedily and transparently through the evaluation of the phase integral $S(x)$, Eq. (4a), between the turning points—zeros of $k^2(x)$—on the farthest potential barriers. The present matching procedure attains the same goal by a substantially equivalent evaluation of the total range of $\phi(x)$ consisting of a sequence of sections separated by matching points x_p. Note, however, that the total range of $S(x)$ in the traditional WKB procedure equals a *half-integer* multiple of π, $(n+\frac{1}{2})\pi$, since each of the exponential tails under the outer barrier contributes a phase $\pi/4$. In the present procedure the *entire* range of $\phi(x)$ amounts to a *whole number* of half-wavelengths.

C. Higher accuracy by WKB iteration

WKB procedures have generally disregarded the last two terms of (9) [or (9a)] which are of second order in the gradient of $\ln h$. However, the combination of (8), (9), and (14) is exactly equivalent to the initial equation (1). An exact solution of (1) becomes accessible by iterating the procedure of Sec. II A, i.e., by taking into account the last two terms of (9) in successive orders of approximation.

This approach has been articulated in detail by Hecht and Mayer.[6] On the other hand the Milne approach to be described in Sec. III leads to a convenient universal calculation of the metric function $h(x)$ as the solution of the single equation (9a) with a preselected $K^2(\phi)$, without resorting to a cumbersome iteration of uncertain convergence.

III. EXACT SOLUTION BY THE MILNE APPROACH

We proceed here beyond the WKB approximation by utilizing the relationship among $K(\phi)$, $k(x)$, and $h(x)$ in its exact form (9) rather than in its WKB form (15) which disregards derivatives of the metric $h=dx/d\phi$. The structure of (9) becomes more transparent when expressed in terms of the derivatives of $h(x)$,

$$\frac{1}{2}h\frac{d^2h}{dx^2}=K^2(\phi)-h^2k^2(x)+\frac{1}{4}\left[\frac{dh}{dx}\right]^2, \tag{22}$$

or of its reciprocal, $g\equiv h^{-1}=d\phi/dx$,

$$\frac{d^2g}{dx^2}=2g\left[k^2(x)-g^2K^2(\phi)+\frac{3}{4}\left[\frac{1}{g}\frac{dg}{dx}\right]^2\right]. \tag{23}$$

A single example will be presented in this section, a wider set in Sec. IV.

Numerical solution of these (nonlinear) equations use Milne's predictor-corrector method (Ref. 17, Eq. 25.5.13ff). This process becomes almost trivial to the extent that proper selection of $K(\phi)$ permits the ratio K/k and hence $g(x)$ to remain nearly constant and smoothly varying over a sizable range of x. The metric functions h or g thus obtained can be parametrized conveniently, e.g., by expansion into a few powers of x. The mosaic procedure of Sec. II B will then combine locally adapted solutions (8) into a complete solution of (1) over the whole range of x.

The flexibility afforded by the constraint (9) has been utilized in part by Milne and his followers[8,9] within the limited context of a sinusoidally varying $Y(\phi)$, in which case

$$K^2(\phi)=1\ . \tag{24}$$

This selection implies that $Y(\phi)\sim\sin\phi(x)$ according to (14), with $\phi(x)=\int^x g(x')dx'$ according to (7). Substituting (24) into (23) and setting $h=\alpha^2$ for convenience yields the analog of (9),

$$d^2\alpha/dx^2+k^2(x)\alpha(x)=1/\alpha^3(x)\ , \tag{25}$$

which is the main equation of Milne.[8] A general solution of this equation involves two integration constants. References 8 and 9 discussed how to select these constants to obtain a generally useful solution over the whole range of x.

In our more general context the solution of (23) may in-

stead by viewed as follows. At an initial point $x=x_0$ [e.g., at a zero or pole of $k(x)$], $K[\int^x dx'g(x')]$ and $g(x)$ are so selected that

$$[k^2(x)-g^2(x)K^2]_{x=x_0}=0\ ,\quad [dg/dx]_{x=x_0}=0\ . \tag{23'}$$

The equation (23) then determines the derivatives of g as k^2 departs from g^2K^2 at finite values of $x-x_0$, beginning with

$$(d^2g/dx^2)_{x=x_0}=0\ . \tag{23''}$$

See note added in proof.

The extended Milne approach described above and the mosaic construction of Sec. II B will now be applied jointly to the double-well problem of Ref. 9, namely, to solve Eq. (1) with

$$k^2(x)=2E-18e^{-x^2}-x^2\ . \tag{26}$$

Figure 1 shows one half plot of the symmetric "potential" $2E-k^2$. Symmetry requires each eigenfunction $y(x)$ to have an antinode or a node at $x=0$; this condition will determine the eigenvalues of E.

Three major features of $2E-k^2$ in (26) stand out, namely, the central hump represented very approximately by $18\exp(-x^2)$, a pair of valleys were $18\exp(-x^2)$ and x^2 are comparable, and a pair of outer parabolic barriers x^2 where $18\exp(-x^2)$ is negligible. We adopt the following three-piece mosaic representation for each half of the potential (26):

(a) $0\le|x|\le 0.7$, where k^2 is very nearly parabolic with vertex at $x=0$;

(b) $0.7\le|x|\le 5$, where k^2 is also nearly parabolic, with opposite curvature and lesser symmetry;

(c) $5\le|x|\le\infty$, where $k^2=2E-x^2$ to within 10^{-12}. The existence of an exact analytic solution at $|x|\ge 5$ reduces the numerical work far below the amount required in Ref. 9.

In each of these ranges the analytical expression (26) is approximated within $\sim 10\%$ by a three-term Taylor expansion

$$k^2(x)=A+B(x-x_0)+C(x-x_0)^2 \tag{27}$$

with the following respective value of $\{A,B,C,x_0\}$:

(a) $A=2E-18$, $B=0$, $C=17$, $x_0=0$;

(b) $A=2E-9.002$, $B=5.99$, $C=-1.038$, $x_0=3$;

(c) $A=2E-25$, $B=-10$, $C=-1$, $x_0=5$.

A smooth metric $g(x)$ is accordingly obtained by starting the solution of (23) at $x=x_0$ in each range. To this end we set in (23)

$$K^2(\phi)=A+B\phi+C\phi^2\ ,\ g(x_0)=1\ , \tag{28}$$

which implies $\phi=x-x_0+O(|x-x_0|^4)$ and satisfies the boundary conditions (23'). The numerical solution $g(x)$ of (23) is plotted in the lower part of Fig. 2 through the ranges (a) and (b). The metric thus constructed separately for each region is generally *discontinuous* at the region boundaries; the wave function is matched at the boundary, but the metric is not. No appreciable departure of $g(x)$ from unit occurred in range (c) where $k^2(x)$ is a parabola as noted above.

Equation (14) with $K^2(\phi)$ of the form (28) is solved by parabolic cylinder functions to be described in Sec. IV B. A base pair of degenerate solutions, even and odd in ϕ, exists whose superposition is dictated by boundary conditions. The relevant condition in range (c), namely, that $Y(\phi)$ vanish at $\phi\to\infty$, identifies $Y(\phi)$ as the convergent Whittaker's function which is a specific superposition of even and odd solutions. Matching logarithmic derivatives of $y(x)$ at the successive boundaries $x=5$ and 0.7 determines in turn the superpositions in the ranges (b) and (a). Lastly, as noted earlier, the solution $y(x)$ must have a node or antinode at $x=0$, a condition that can now be met only by adjusting the value of E in (26).

Comparison with the results of Ref. 9 is shown by the listing of eigenvalues in Table I. The agreement of eigenvalues contrasts with the modest accuracy of the representation of $k^2(x)$ by (27). The semianalytic treatment utilized here has made it possible to use a mesh of $\Delta x=0.1$ whereas $\Delta x=0.01$ was required in Ref. 9 to avoid instabilities in the analog of (23) for $Y=\sin\phi$ over the whole range of x. Figure 2 shows a sample of eigenfunctions

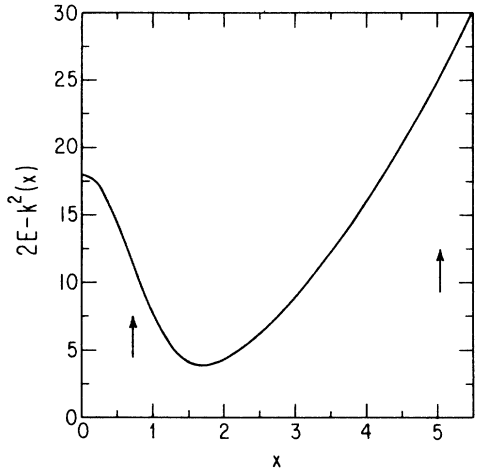

FIG. 1. Potential Function $2E-k^2(x)$ for Eq. (26) and $x\ge 0$.

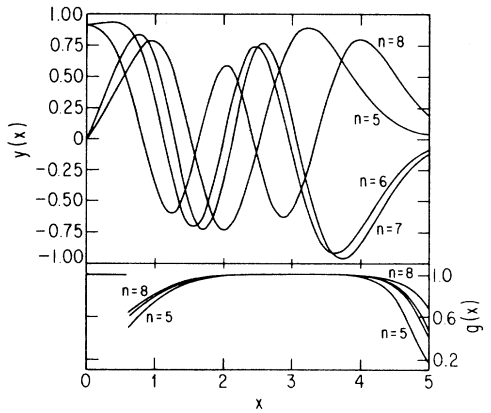

FIG. 2. Wave functions $y(x)$, with 5,6,7,8 nodes, and metrics $g(x)$ calculated by the extended Milne method for the $k^2(x)$ of Eq. (26). The metric functions $g(x)$ is discontinuous at the section boundaries. The magnitude and slope of the wave functions are instead matched at the boundaries.

TABLE I. Eigenvalues for the double well, Eq. (24).

Nodes	Ref. 9	Extended Milne	
n	$\Delta x=0.01$	$\Delta x=0.1$	$\Delta x=0.05$
0	3.075 395	3.075 414	
1	3.078 507	3.078 525	
2	5.138 300	5.138 315	
3	5.164 373	5.164 383	
4	6.971 396	6.971 422	
5	7.098 398	7.098 423	7.098 3985
6	8.576 210	8.576 236	8.576 2095
7	8.967 876	8.967 902	8.967 8749
8	10.122 34	10.122 33	10.122 324

$y(x)$ with different degrees of penetration through the barrier between the wells.

IV. ILLUSTRATIONS

Physical and mathematical aspects of familiar wave equations will be illustrated in this section by combining the devices introduced above to represent qualitative and quantitative features of one-dimensional wave functions, namely, the following.

(1) Choice of analytic functions $Y(\phi)$ whose squared wave number $K^2(\phi)$ embodies characteristic nodes and/or poles of $k^2(x)$.

(2) Scaling adaptation of the phase ϕ and the amplitude of Y to fit the actual wave function $y(x)$ of a specific equation over a significant range of x. [An approximate fit is provided by the simple equation (17) or (18), an exact fit by numerical solution of the Milne equations (22) or (23) for a smooth metric function.]

(3) Construction of a desired function $y(x)$ as a mosaic of analytic functions $Y(\phi)$ appropriate to represent its main features in different ranges of x.

A. Transition from oscillation to tunneling—Airy functions

The oscillatory and tunneling ranges of a WKB solution, Eqs. (5a) and (5b), are separated by a node of $k^2(x)$. Formulas that connect these WKB solutions[2] assumed that $k^2(x)$ varies linearly over a sufficient range of x astride its node. This procedure is implemented in our context by utilizing a *single solution* of (14) across the node of $k^2(x)$, setting $K^2(\phi)$ linear in ϕ and anchoring ϕ at zero at the node of k^2. The resulting form of (14), with $K^2(\phi)=\phi$, coincides with the model equation (Ref. 17, Eq. 10.4, with $z=-\phi$),

$$d^2Y/d\phi^2+K^2(\phi)Y=d^2Y/d\phi^2+\phi Y(\phi)=0\ , \tag{29}$$

which is obeyed by the Airy function

$$Y(\phi)=\mathrm{Ai}(-\phi) \tag{30}$$

and is plotted in Fig. 3.

The mapping (7) of the phase function $\phi(x)$ on the coordinate x anchors the value $\phi=0$ to the node of $k^2(x)$ at $x=x_0$. The WKB approximation sets, more specifically,

$$S(x)=\int_{x_0}^{x}k(x')dx'=\int_0^{\phi}\phi'^{1/2}d\phi'=\tfrac{2}{3}\phi^{3/2}\ . \tag{31}$$

It is assumed here that $k^2(x)>0$ for $x>x_0$, $S(x)$ and ϕ being then real and positive in this range. For $x'<x_0$, on the other hand we have $k^2(x)<0$ and $\phi<0$, and hence $\mathrm{Im}k(x')<0$ and $\mathrm{Im}S(x)<0$ as well as $\mathrm{Re}k(x')=\mathrm{Re}S=0$.

This mapping is accurate insofar as $k^2(x)$ remains proportional to $x-x_0$ implying that $h(x)=\phi^{1/2}/k(x)=$constant. In this event the asymptotic expressions of $Y(\phi)$ at $\phi\to\infty$ (Ref. 17, Eq. 10.4.62) coincide with the WKB expressions (4a) and (4b). For purposes of comparison the mapping of ϕ on $x-x_0$ has been calculated for $k^2(x)=x-x_0+(x-x_0)^3/10$, using alternatively the WKB Eq. (17) or a solution of the exact Eq. (22) for the metric $h(x)$, with the results shown in Fig. 3.

Equation (27) has a second standard solution independent of $\mathrm{Ai}(-\phi)$, which is called $\mathrm{Bi}(-\phi)$ and diverges at $\phi\to-\infty$. This solution should generally be superposed to $\mathrm{Ai}(-\phi)$ not only when $k^2(x)$ becomes again positive in the range $x<x_0$, but also when the metric $h(x)$ calculated from (22) or (23) departs from its WKB approximation (17).

B. Minima and maxima of $k^2(x)$—parabolic cylinder functions

The analytic significance of extrema of the wave number has been indicated at the end of Sec. II A. In the proximity of this type of singularity a wave equation may be cast in the standard form (Ref. 7, Chap. 19),

$$d^2Y/d\phi^2+K^2(\phi)Y=d^2Y/d\phi^2+(\pm\phi^2/4-a)Y(\phi)=0\ . \tag{32}$$

The parameter $-a$ represents the value of $K^2(0)$, which is positive when $Y(\phi)$ oscillates in the range $|\phi|\sim 0$, nega-

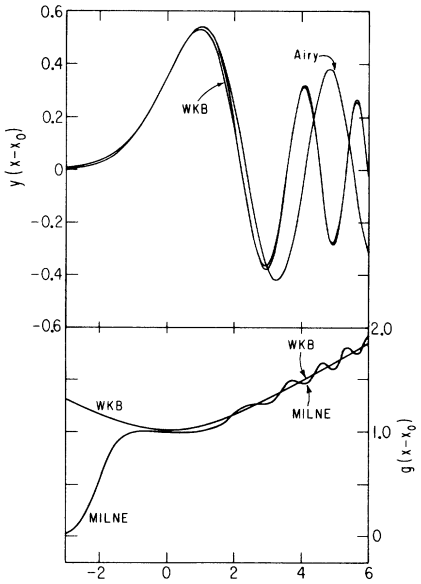

FIG. 3. Wave functions $y(x)$ and metric $g(x)$ for $k^2(x)=(x-x_0)+(x-x_0)^3/10$ calculated by the extended Milne and extended WKB methods. Also shown, for comparison, is the Airy function $\mathrm{Ai}(x_0-x)$.

tive when it is tunneling through a barrier in this range.

A negative sign of $\phi^2/4$ in (32) implies negative values of $K^2(\phi)$ for large $|\phi|$, in which case oscillations of Y are confined to a range about $\phi=0$ and the eigenvalue spectrum of (32) is discrete (Fig. 4). A positive sign of $\phi^2/4$ implies instead large positive value of $K^2(\phi)$ and increasingly short-wave oscillations of $Y(\phi)$ at large $|\phi|$, in which case the eigenvalue spectrum is continuous with degenerate eigenfunctions of even and odd parity about $\phi=0$. Two quite different types of wave phenomena are thus represented by solutions of (32), which we will call "valley" and "barrier" solutions and correspond to minima and maxima of $k^2(x)$, respectively.

Both types of solutions are known as parabolic cylinder functions and are represented analytically as Coulomb field wave functions of ϕ^2, that is, in terms of confluent hypergeometric functions $M(p,q;x)=1+px/q+p(p+1)x^2/q(q+1)2!+\cdots$. Valley and barrier solutions of (32) with alternative parity are

$$Y_v^e(\phi)=e^{-\phi^2}M(\tfrac{1}{2}a+\tfrac{1}{4},\tfrac{1}{2};2\phi^2)\,, \tag{33a}$$

$$Y_v^o(\phi)=\phi e^{-\phi^2}M(\tfrac{1}{2}a+\tfrac{3}{4},\tfrac{1}{2};2\phi^2)\,, \tag{33b}$$

$$Y_b^e(\phi)=e^{-i\phi^2}M(-\tfrac{1}{2}ia+\tfrac{1}{4},\tfrac{1}{2};2i\phi^2)\,, \tag{34a}$$

$$Y_b^o(\phi)=\phi e^{-i\phi^2}M(-\tfrac{1}{2}ia+\tfrac{3}{4},\tfrac{1}{2};2i\phi^2)\,, \tag{34b}$$

all of which are real. The valley solutions Y_v are oscillator-type wave functions; they coincide with oscillator eigenfunctions when $\frac{1}{2}a+\frac{1}{4}$ or $\frac{1}{2}a+\frac{3}{4}$ is a nonpositive integer and $M(p,q;2\phi^2)$ reduces to a polynomial. The barrier solutions Y_b tunnel between nodal points at $\phi=\pm(4a)^{1/2}$ for $a>0$, but oscillate everywhere when the minimum of $k^2(x)$ is non-negative.

Departures of $k^2(x)$ from a parabola skew, or otherwise distort, the mapping of ϕ on x. Examples of the mapping have been worked out for $k^2(x)=a+(x-x_0)^2/4+(x-x_0)^3/b$, again both in the WKB approximation (17) and by solving (22) (Fig. 5). These mappings reflect the asymmetry of $k^2(x)$ under reflection through x_0. Recall

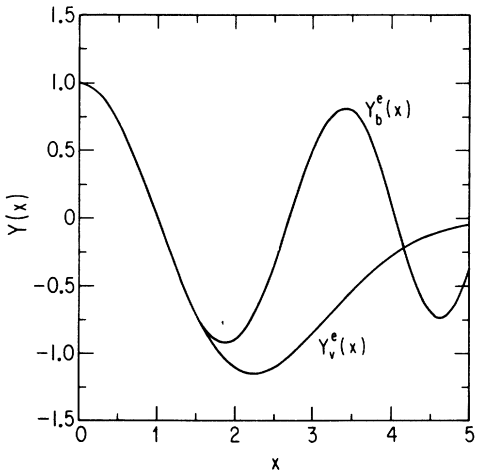

FIG. 4. Valley and barrier parabolic cylinder functions with $a=-\frac{5}{2}$ and $\phi\geq 0$.

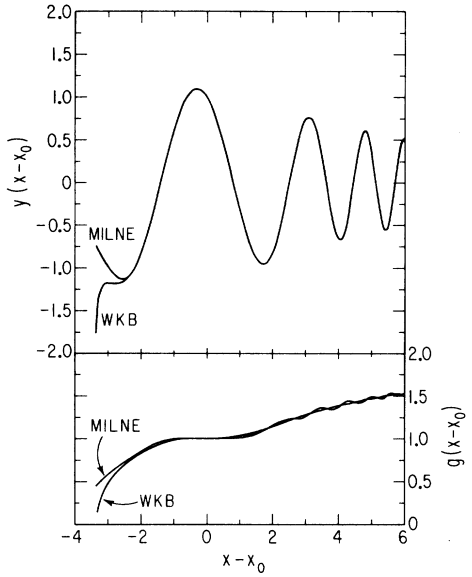

FIG. 5. Same as Fig. 3 for $k^2(x)=2+(x-x_0)^2/4+(x-x_0)^3/10$ using the appropriate parabolic cylinder function. Note the asymmetry introduced by the cubic term.

here that the mapping through the WKB approximate Eq. (17) implies cancellation of the singularities of K and k in their ratio.

Symmetry of a barrier about its peak—a minimum of $k^2(x)$—serves, on the other hand, to evaluate the reflection coefficient of the barrier for an incident wave. Superposition of the degenerate functions Y_b of opposite parity generates traveling waves which are partly reflected. The Landau-Zener-Stückelberg formula,[18] which governs the nonadiabatic transitions in atomic collisions at avoided level crossings, rests in fact on this procedure for the case of $k^2(x)$ symmetric about its minimum. Its applications could be extended considerably by flexible mapping of x on $\phi(x)$.

Asymptotic expressions of the wave functions (33) and (34), or of the corresponding $(dx/d\phi)^{1/2}Y_v$, reduce to the WKB forms (4) or (5), as can be verified, e.g., from Ref. 17, Eqs. 19.8 and 19.21. For large values of the parameter $|a|$, in which case the nodes of $k^2(x)$ are widely separated, the solutions $y(x)$ of (1) could also be approximated by Airy functions near each node. Indeed expansions of the solutions Y_v and Y_b directly into Airy functions are available (Ref. 17, Eqs. 19.7 and 19.20).

An example of analytical mosaic solution of the wave equation (1) is afforded by a functional form of $k^2(x)$ that consists of two parabolic sections with one maximum and one minimum, respectively,

$$\begin{aligned} k^2(x)&=-(x+b)^2/4+b^2/4+c\,, \quad x\leq 0 \\ k^2(x)&=(x-b)^2/4-b^2/4+c\,, \quad x\geq 0\,. \end{aligned} \tag{35}$$

The mapping of ϕ on x is then

$$\phi=-(x+b) \text{ for } x\leq 0\,, \quad \phi=x-b \text{ for } x\geq 0 \tag{36}$$

with $h=1$ and $y=Y$. Wave functions (33) and (34) that meet all the boundary conditions are determined in the Appendix and shown in Fig. 6.

Further applications of parabolic cylinder functions will occur below, in the construction of oblate spheroidal functions (Sec. IV C) and of Stark effect wave functions (Sec. IV D).

C. Pole singularity of centrifugal origin—Bessel functions

Singularities generally occur in one-dimensional wave equations originating from the separation of a multidimensional equation in polar or other noncartesian coordinates. Separation in cylindrical coordinates (ρ,z), leading to the Bessel equation with a regular singular point at $\rho=0$, serves as prototype bearing on other applications. The Bessel equation proper includes a first-derivative term whose elimination leads to the modified equation

$$\left[\frac{d^2}{d\rho^2}+\left[1-\frac{m^2-\frac{1}{4}}{\rho^2}\right]\right]\bar{J}_m(\rho)=0\ , \tag{37}$$

for the modified Bessel function $\bar{J}_m(\rho)=\sqrt{\rho}J_m(\rho)$ which

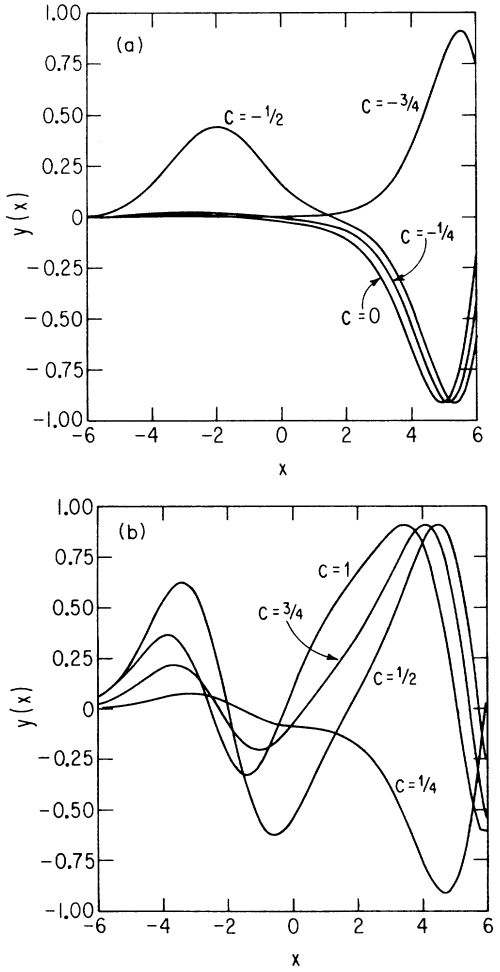

FIG. 6. Wave functions for the $k^2(x)$, Eq. (35), with $b=-2$ and energy values c yielding a resonance and other effects of a potential barrier.

serves as a prototype $Y(\phi)$ in the following.

As a preface to extended use of (37) note that replacing the coefficient 1 by a constant β^2 would simply change $\bar{J}_m(\rho)$ into $\bar{J}_m(\beta\rho)$, through division of the equation by β^2. Problems of interest involve, however, replacing 1 by a slowly variable coefficient $\beta^2(\rho)$, much as WKB applications replace the unit coefficient of the trigonometric equation by a slowly varying coefficient $k^2(x)$. The equation has now the form (1) with the coefficient

$$k^2(x)=\beta^2(x)-\frac{m^2-\frac{1}{4}}{x^2}\ , \tag{38}$$

which combines a smooth term $\beta^2(x)$ with the singular term $\propto 1/x^2$. We proceed to take into account the singular term analytically by the transformations (7), where we set $Y(\phi)\equiv\bar{J}_m(\phi)$ and accordingly

$$K^2(\phi)=1-(m^2-\tfrac{1}{4})/\phi^2\ . \tag{39}$$

The process is completed by entering the expressions (38) and (39) of k^2 and K^2 in (9b) and solving this equation for the metric coefficient $h(x)$. The WKB approximation (17) to this equation yields

$$h(x)=\frac{dx}{d\phi}=\left[\frac{1-(m^2-\frac{1}{4})/\phi^2}{\beta^2(x)-(m^2-\frac{1}{4})/x^2}\right]^{1/2}\ . \tag{40}$$

Note how the singularities of (40) at $x=\phi=0$ clearly cancel; the connection (40) between the scales of ϕ and x also requires the zeros of its numerator and denominator to coincide.

An analogous pole of centrifugal origin emerges from the separation of wave equations in spherical polar coordinates which leads to the equation for the associate Legendre functions

$$\left[\frac{d^2}{d\theta^2}+\cot\theta\frac{d}{d\theta}+l(l+1)-\frac{m^2}{\sin^2\theta}\right]P_{lm}(\theta)=0\ . \tag{41}$$

A first-derivative term appears here, as it does in the Bessel equation. To eliminate this term, as in the construction of (37), one replaces P_{lm} by $\bar{P}_{lm}(\theta)=(\sin\theta)^{1/2}P_{lm}(\theta)$. The corresponding substitution $P_{lm}=(\sin\theta)^{-1/2}\bar{P}_{lm}$ reduces (41) to

$$\left[\frac{d^2}{d\theta^2}+k_{lm}^2(\theta)\right]\bar{P}_{lm}(\theta)=0 \tag{42}$$

with

$$k_{lm}^2(\theta)=(l+\tfrac{1}{2})^2-(m^2-\tfrac{1}{4})/\sin^2\theta\ . \tag{43}$$

This expression of k_{lm}^2, with a pole $\propto 1/\theta^2$, is now equivalent to that of $k^2(x)$ in (38). We thus obtain the final expression of a spherical harmonic in terms of a Bessel function

$$P_{lm}(\theta)=(\sin\theta)^{1/2}\bar{P}_{lm}(\theta)=\left[\frac{h(\theta)}{\sin\theta}\right]^{1/2}\bar{J}_m(\phi)\ , \tag{44}$$

where the metric $h(\theta)$ is the solution of (22) with $K^2(\theta)$ from (39) and $k^2(x)$ replaced by $k_{lm}^2(\theta)$. The WKB approximation yields instead

TABLE II. Calculated eigenvalues for $\bar{P}_{lm}$, Eq. (42).

l	m	Meshpoint no.	$(l+\frac{1}{2})^2$
1	0	4	2.25002
1	0	10	2.2500001
2	0	5	6.25008
3	0	5	12.2504
4	0	10	20.2504
5	0	10	30.24997
1	1	5	2.25001
2	1	5	6.25005
3	1	5	12.2501
4	1	10	20.250007

$$h(\theta)=\frac{d\theta}{d\phi}=\left[\frac{1-(m^2-\frac{1}{4})/\phi^2}{(l+\frac{1}{2})^2-(m^2-\frac{1}{4})/\sin^2\theta}\right]^{1/2} . \quad (45)$$

Operation of the Milne technique is demonstrated here by calculating the eigenvalues and eigenfunctions of (42) and (43) and comparing them with their familiar expressions, $(l+\frac{1}{2})^2$ and $\bar{P}_{lm}(\theta)$. To this end we rewrite (43) as $k^2(\theta)=E-(m^2-\frac{1}{4})/\sin^2\theta$, where E is the eigenvalue to be determined. We also minimize the variation of the ratio ϕ/θ by setting

$$K^2(\phi)=E-(m^2-\tfrac{1}{4})(1/\phi^2-\tfrac{1}{3}) , \quad (46)$$

which matches the first two terms of the power expansion of $k^2(\theta)$, yielding $\phi=\theta+O(\theta^5)$. Equation (23) is now entered at $\theta=0$ with $\phi(0)=0$, $g(0)=1$, $g'(0)=0$, and is propagated to $\theta=\pi/2$ by Milne's predictor-corrector method (Ref. 17, 25.5.13ff). We determine the value of E by requiring that either

$$y(\theta)=[g(\theta)\sin\theta]^{-1/2}\bar{J}_m\{[E-(m^2-\tfrac{1}{4})/3]^{1/2}\phi(\theta)\} \quad (47)$$

or $dy/d\theta$ vanishes at $\theta=\pi/2$. Table II shows eigenvalues determined by this method and the number of mesh points used in propagating (23) from 0 to $\pi/2$. Figures 7 and 8 show values of $y(\theta)$ and $g(\theta)$. Representative values of the ratios $y(\theta)/\bar{P}_{lm}(\theta)$ depart from a constant in the fifth or sixth digit. Note how $g(\theta)$ becomes smoother as l increases, in contrast to the increasing curvature of $y(\theta)$.

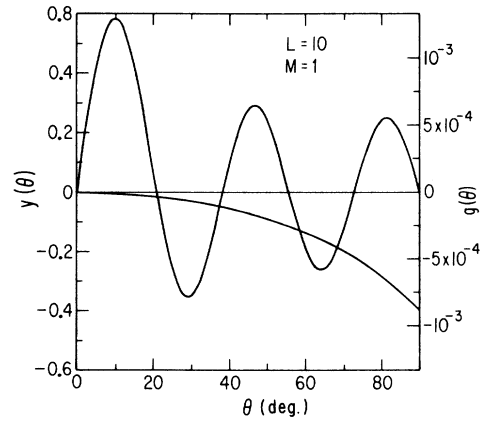

FIG. 7. Associated Legendre function $P_{l,m}(\theta)$ and the corresponding metric $g(\theta)$ calculated by the extended Milne method.

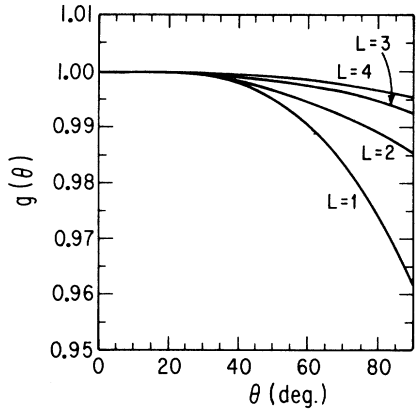

FIG. 8. Metrics $g(\theta)$ for various $P_{l,1}(\theta)$, as in Fig. 7.

Combination of Milne and mosaic procedures is documented by generating the oblate spheroidal functions indicated by $S_{mn}(c,\cos\theta)$ in Ref. 17, Eq. 21.6.4. The equation for $\bar{S}_{mn}(c,\cos\theta)=(\sin\theta)^{1/2}S_{mn}(c,\cos\theta)$ has the form (42) with k_{lm}^2 replaced by

$$k_{mn}^2=\lambda_{mn}+c^2-c^2\sin^2\theta-\frac{m^2-\frac{1}{4}}{\sin^2\theta} , \quad (48)$$

the main additional feature being the insertion of a barrier centered at $\theta=\pi/2$. This insertion leads us to separate the range $0\le\theta\le\pi/2$ into two sections of a mosaic representation: (a) The representation (47) will again apply for small values of θ, say $0\le\theta<\pi/6$, where the centrifugal term of (48) predominates over $c^2\sin^2\theta$; (b) a representation $h^{1/2}(\theta)Y_b(\phi)$ with parabolic cylinder functions (34) will instead apply to the range of larger θ where the barrier term of (48) predominates.

The relationship between ϕ and θ in range (b) is smoothed out by utilizing a quadratic form of $K^2(\phi)$ which matches a three-term expansion of (48) into powers

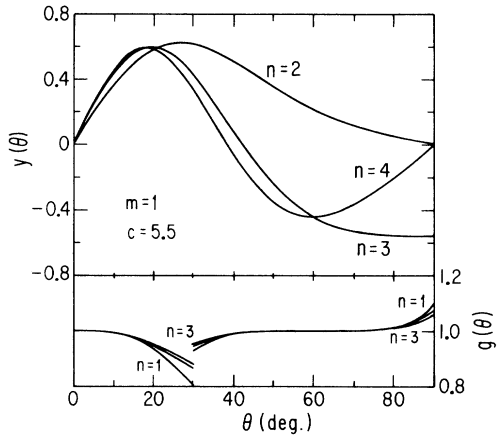

FIG. 9. Oblate spheroidal functions $\bar{S}_{m,n}$ and their metrics $g(\theta)$ calculated from Eq. (48) by the extended Milne method with a two-section mosaic.

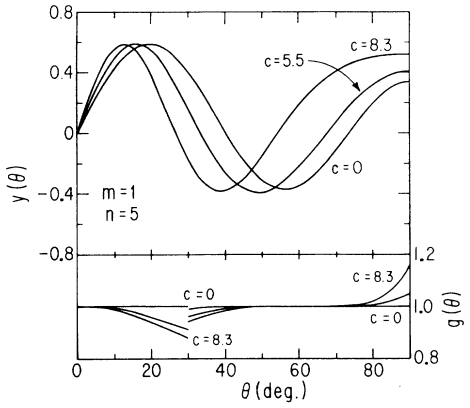

FIG. 10. Same as Fig. 9 for different values of c.

of $(\theta-\theta_0)$ with θ_0 in the middle of this range. The solution of (23) starts then at $\theta=\theta_0$ with $g(\theta_0)=1$, $g'(\theta_0)=0$ and propagates thence in both directions. The zero of ϕ is anchored at θ_0 by defining

$$\phi(\theta)=\int_{\theta_0}^{\theta} g(\theta')d\theta' \ . \tag{49}$$

The occurrence of an antinode or a node of $y(\theta)$ at $\theta=\pi/2$ is enforced by constructing the appropriate superposition of $h^{1/2}Y_b^e(\phi)$ and $h^{1/2}Y_b^o(\phi)$ from (34).[19] The eigenvalue $\lambda_{mn}+c^2$ in (48) is instead determined in this case by matching $d\ln y/d\theta$ at the boundary of the two-section mosaic representation.

Results of the calculation are presented in Figs. 9 and 10, for fixed $c=5.55$ and variable n or for $n=5$ and variable c, respectively. Note the limited ranges of smooth variation of $g(\theta)$. Table III compares instead the eigenvalues calculated by the present and by standard procedures and gives sample ratios of the corresponding

TABLE III. Calculated eigenvalues, $\lambda_{m,n}$, for $\bar{S}_{m,n}(c,\cos\theta)$.

	$m=1$, $n=5$	
c	(Ref. 17)	Extended Milne
0	30.25	30.2500
5.55	47.0648	47.0652
8.33	72.965	72.973

	$c=5.555$, $m=1$	
n	(Ref. 17)	Extended Milne
2	20.2987	20.2988
3	32.323	32.323
4	37.265	37.265

Calculated ratio $\dfrac{\bar{S}_{1,5}(0,\cos,\theta)}{\bar{P}_{51}(\cos\theta)}$ (not normalized)

30°	45°	60°	90°
3.102 448	1.102 450	3.102 449	3.102 451

values of the eigenfunctions $y(\theta)$.

D. Coulomb-type pole: Bessel functions again

The radial factor of the Schrödinger equation for a hydrogenic atom with orbital quantum number l has the form (1) with the squared wave number

$$k_l^2(r)=\beta^2+\frac{a}{r}-\frac{l(l+1)}{r^2} \ . \tag{50}$$

To assess the specific influence of the Coulomb pole, consider the phase integral

$$S_0(r)=\int_0^r dr' k_0(r')=2\int_0^{\sqrt{r}} d\sqrt{r'}(\beta^2 r'+a)^{1/2} \tag{51}$$

for $l=0$ and note that it remains finite in spite of the singularity of k_0. This integration procedure suggests replacing the coordinate r at the outset by its square root, through the transformation (7)—(9), which reads in this case

$$r\rightarrow\phi=\sqrt{r} \ , \quad h=dr/d\phi=2\sqrt{r} \ , \quad Y(\phi)=(4r)^{-1/4}y(r) \ , \tag{52}$$

$$K_l^2(\phi)=4r\left[\beta^2+\frac{a}{r}-\frac{l(l+1)}{r^2}-\frac{1}{4r^2}+\frac{1}{16r^2}\right]$$

$$=4(\beta^2\phi^2+a)-\frac{(2l+1)^2-1/4}{\phi^2} \ . \tag{53}$$

Note that (53) includes substantial contributions from the derivatives in (9b).

Consider now the wave equation (14) for $Y(\phi)$ with the coefficient $K_l^2(\phi)$ given by (53), initially for the special case $\beta^2=0$ which corresponds to a zero-energy eigenvalue of the Schrödinger equation. Comparison with the Bessel equation (37) shows the zero-energy eigenfunction to be

$$Y_l(\phi)=(\sqrt{4a}\,\phi)^{1/2}\bar{J}_{2l+1}(\sqrt{4a}\,\phi) \ , \tag{54}$$

a long-known result.[20] The important point in our context is that the wave equation will remain smoothly dependent on ϕ even for a smoothly varying $\beta^2(\phi^2)\neq 0$. Accordingly the Schrödinger equation (1) with the wave number k_l^2 (50) can be solved semianalytically in terms of a Bessel function for *nonzero energies*, through a further transformation of the variable ϕ.[4] The same procedure applies to a radial equation with a potential that departs from the Coulomb law by introducing in (50) a nonsingular $2Z(r)$ in place of the constant a. This implication of Langer's original work does not seem to have attracted attention.

We illustrate now the Bessel representation of a radial wave function $y_l(r)$ for an atomic field by entering in (50) $\beta^2=0.2$, corresponding to the electron energy of 0.1 atomic units, $l=0$ and $a=2Z(r)$ with $Z(r)$ the Hartree-Slater atomic parameter for the Ar atom.[21] The representation $y_l(r)=h^{1/2}\bar{J}_{2l+1}(\phi)$ requires us to set $K_l^2(\phi)=1-[(2l+1)^2-\frac{1}{4}]/\phi^2$. The metric h that connects ϕ to r is then provided by (17) and (18) in the WKB approximation or by solving (22) or (23) in the Milne approach. Figure 11 shows the result thus obtained by solving (23) as well as the resulting wave function $y_l(r)$, which does not depart

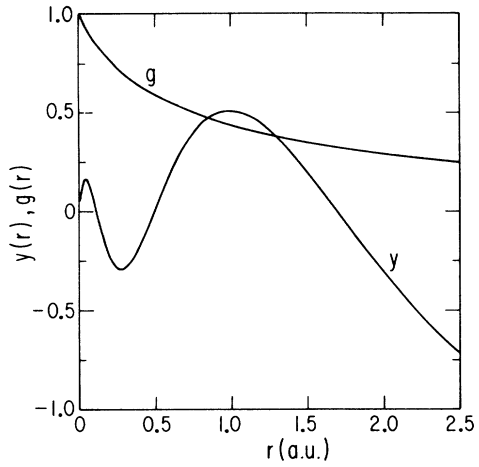

FIG. 11. Bessel function representation of the radial wave function of an ionic state of argon with $l=0$ and energy 0.1 a.u. The Herman-Skillman potential was given numerically.

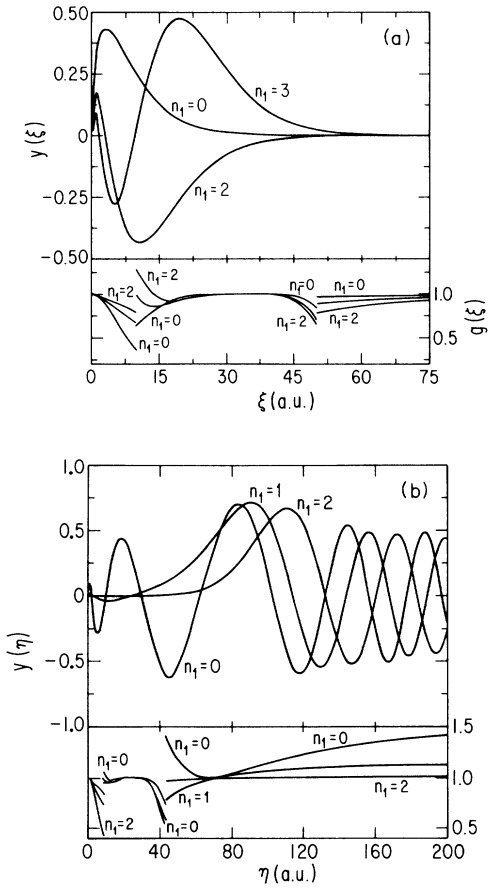

FIG. 12. Stark effect wave functions of a hydrogen atom in parabolic coordinates for a field $F=0.001$ a.u. $\sim 10^4$ V/cm, energy $\varepsilon=-0.05$ a.u., and $m=0$ in Eqs. (55) and (56). (a) Wave functions $y(\xi)$ with n_1 nodes and metrics $g(\xi)$. (b) Wave functions $y(\eta)$ and metrics $g(\eta)$ with β_1 eigenvalues corresponding to n_1 and given in Table IV.

significantly from the direct numerical solution of the Schrödinger equation. The construction of $y_l(r)$ has utilized here the expression $h^{1/2}\bar{J}_{2l+1}(\phi)$ throughout the range of r, but a mosaic utilizing an additional Airy function would be required to represent a bound state with $\beta^2<0$.

As a final illustration we rederive results of Harmin on the Stark effect of the H atom near its ionization threshold.[22] The relevant wave equation separates in parabolic coordinates $\{\xi=r+z,\eta=r-z,\phi\}$. Here we consider the ξ and η components of the equation which are represented by (1) with[22]

$$k^2(\xi)=\frac{1}{2}\varepsilon+\frac{\beta_1}{\xi}-\frac{m^2-\frac{1}{4}}{\xi^2}-\frac{F}{4}\xi \tag{55}$$

and

$$k^2(\eta)=\frac{1}{2}\varepsilon+\frac{1-\beta_1}{\eta}-\frac{m^2-\frac{1}{4}}{\eta^2}+\frac{F}{4}\eta\ , \tag{56}$$

respectively. The electron energy ε, in atomic units, has a continuous spectrum in this problem, the magnetic quantum number m is an integer, and F is the Stark field strength whose value $\sim 10^{-5}$ corresponds to $\sim 10^4$ V/m. The separation parameter β_1 is determined as an eigenvalue for the motion along ξ which is bounded by the Stark field in the direction $\xi\to\infty$ in contrast to the unbounded motion toward $\eta\to\infty$.

The influence of the Coulomb and centrifugal singularities in both (55) and (56) is to be incorporated here into a Bessel function $\bar{J}_{2m}(\phi)$ representation, for both coordinates ξ and η, in contrast to Harmin's use of WKB phase integrals supplemented by Langer corrections. The bounded propagation at large ξ—limited by the rising potential term $-F\xi/4$—is to be represented here through an Airy function whose matching into a mosaic determines the eigenvalues β_1. The mosaic consists of three sections, including a central one, where the potential is nonsingular but with substantial curvature. The wave function in the central section is then represented by a parabolic cylinder $Y_v(\phi)$. The propagation along η in the region of the maximum of $\varepsilon/2-k^2(\eta)$, at $\eta\sim 4(1-\beta_1)/F$, is to be treated according to (20) as penetration through or above a parabolic barrier, represented by a wave function $Y_b(\phi)$, Eq.

TABLE IV. Eigenvalue of Eq. (55) and phase shift of Eq. (57).

	β_1 ($F=0.001$, $\varepsilon=-0.05$)		
	$n_1=0$	$n_1=1$	$n_1=2$
Ref. 22[a]	0.1619	0.5081	0.8843
Extended Milne	0.1615	0.5033	0.8696
	δ ($F=0.001$, $\varepsilon=-0.05$)		
	$n_1=0$	$n_1=1$	$n_1=2$
Ref. 22	6.65	3.86	0.37
Extended Milne	6.65	3.85	0.35

[a]Data from Ref. 22 have been calculated as a small perturbation from its $F=0$ Eq. 55. The Milne values may be more accurate especially for $n_1=2$.

(34). Its propagation at $\eta \sim 0$ is represented again by a $J_{2m}(\phi)$. Finally, the term $F\eta/4$ of (56) predominates at large η leading to a third local representation of $y(\eta)$,

$$h^{1/2}(\eta)[\cos\delta\,\mathrm{Ai}(-\phi)+\sin\delta\,\mathrm{Bi}(-\phi)]\ , \tag{57}$$

ϕ being in this case exactly proportional to η in the limit $\eta \to \infty$. The resulting wave functions and metrics g are shown in Fig. 12, the comparison of parameters with those of Ref. 22 in Table IV.

Note added in proof. This choice of boundary conditions, called WKB boundary conditions by B. Yoo and C. H. Greene, Phys. Rev. A **34**, 1635 (1986), leads to the small-amplitude oscillations of $g(x)$ shown in Figs. 3 and 5. Yoo and Greene describe a procedure for eliminating these oscillations.

ACKNOWLEDGMENTS

We are indebted to David de Mille and Noah Butter for extensive work that led to the present paper and to A. R. P. Rau for stressing the opportunity of combining WKB and Milne approaches. This work has been supported by the U.S. Department of Energy, Office of Basic Energy Sciences.

APPENDIX

A general solution of the wave equation (1) with

$$\begin{aligned} k^2(x) &= \frac{-(x+b)^2}{4}+b^2/4+c\ , \quad x\le 0 \\ &= \frac{(x-b)^2}{4}-b^2/4+c\ , \quad x\ge 0 \end{aligned} \tag{A1}$$

is

$$\begin{aligned} y(x) &= C_v^e Y_v^e(x+b)+C_v^o Y_v^o(x+b)\ , \quad x\le 0 \\ &= C_b^e Y_b^e(x-b)+C_b^o Y_b^o(x-b)\ , \quad x\ge 0\ . \end{aligned} \tag{A2}$$

Its coefficients C are determined by the constraints (a) $y(x)$ must not diverge as $x\to-\infty$, (b) $y(x)$ must be continuous at $x=0$, (c) dy/dx must be continuous at $x=0$. These constraints determine all of the coefficients to within normalization. The first condition is satisfied when $y(x)$ coincides with Whittaker's convergent function (Ref. 17, 19.3.1), the coefficients being then $C_v^e = 1/\Gamma(\frac{3}{4}-c/2-b^2/8)$, $C_v^o = \sqrt{2}/\Gamma(\frac{1}{4}-c/2-b^2/8)$. The last two constraints give

$$\begin{aligned} &C_v^e Y_v^e(b)+C_v^o Y_v^o(b) = C_b^e Y_b^e(b)-C_b^o Y_b^o(b)\ , \\ &C_v^e Y_v^{e\prime}(b)+C_v^o Y_v^{o\prime}(b) = -C_b^e Y_b^{e\prime}(b)+C_b^o Y_b^{o\prime}(b)\ , \end{aligned} \tag{A3}$$

which finally yields

$$\begin{aligned} C_b^0 &= Y_b^{e\prime}(b)\frac{C_v^e Y_v^e(b)+C_v^o Y_v^o(b)}{Y_b^{0\prime}(b)Y_b^e(b)-Y_b^{e\prime}(b)Y_b^o(b)} \\ &\quad + Y_b^e(b)\frac{C_v^e Y_v^{e\prime}(b)+C_v^o Y_v^{o\prime}(b)}{Y_b^{o\prime}(b)Y_b^e(b)-Y_b^{e\prime}(b)Y_b^o(b)} \\ &= Y_b^{e\prime}(b)[C_v^e Y_v^e(b)+C_v^o Y_v^o(b)] \\ &\quad + Y_b^e(b)[C_v^e Y_v^{e\prime}(b)+C_v^e Y_v^{o\prime}(b)] \end{aligned} \tag{A4}$$

and

$$C_b^e = [C_v^e Y_v^e(b)+C_v^o Y_v^o(b)+C_b^o Y_b^o(b)]/Y_b^e(b)\ .$$

---

*Present address: Department of Physics and Astronomy; University of Nebraska, Lincoln, NE 68588-0111.

[1]The symbol JWKB is often used to recognize an earlier contribution by Jeffreys.

[2]H. A. Kramers, Z. Phys. **39**, 826 (1926).

[3]C. Lanczos, Z. Phys. **62**, 518 (1930); **68**, 204 (1931). This work contains the germ of most later developments.

[4]R. E. Langer, Phys. Rev. **51**, 669 (1937). The first portion of this paper is most widely known, but its last part has proved most relevant to the present work.

[5]S. C. Miller and R. H. Good, Phys. Rev. **91**, 174 (1953). This work introduced the systematic application of Eq. (18).

[6]C. E. Hecht and J. E. Meyer, Phys. Rev. **106**, 1156 (1957). This work also exploits much of our mathematical tools for a restricted purpose.

[7]B. Durand and L. Durand, Phys. Rev. A **33**, 2887 (1986).

[8]W. E. Milne, Phys. Rev. **35**, 863 (1930); E. Young, *ibid.* **38**, 1613 (1931); **39**, 445 (1932); J. C. Wheeler, *ibid.* **52**, 1123 (1937).

[9]H. J. Korsch and H. Laurent, J. Phys. B **14**, 4213 (1981).

[10]C. H. Greene, A. R. P. Rau, and U. Fano, Phys. Rev. A **26**, 2441 (1982).

[11]U. Fano in *Semiclassical Description of Atomic and Nuclear Collisions,* edited by J. Bang and J. de Boer (Elsevier, New York, 1985).

[12]P. Pechukas, J. Chem. Phys. **57**, 5577 (1972); N. De Leon and E. J. Heller, Phys. Rev. A **30**, 5 (1984).

[13]In wave mechanics the WKB procedure is often introduced as an expansion of the Schrödinger equation into powers of $\hbar$. In fact $\hbar$ plays only the role of a dimensional constant in the operator $p=-i\hbar(d/dx)$, but $\hbar$ is incorporated in $k(x)$ in the more general Eq. (1).

[14]R. Courant and D. Hilbert, *Methods of Mathematical Physics* (Interscience, New York, 1953), Vol. I. Chap. 4.

[15]Centrifugal potentials emerge generally from the Jacobian derivative $\partial(x,y,z)/\partial(\xi,\eta,\zeta)$ of the transformation of a multidimensional analog of the variational integral (6). See, e.g., Ref. 14, Sec. 4.8.

[16]K. Smith, *The Calculation of Atomic Collision Processes* (Wiley, New York, 1971).

[17]M. Abramowitz and I. A. Stegun, *Handbook of Mathematical Functions* (Dover, New York, 1972)

[18]L. D. Landau, Phys. Z. Sovjetunion **2**, 46 (1932); C. Zener, Proc. R. Soc. (London), Ser. A **137**, 696 (1932); E. L. G. Stückelberg, Helv. Phys. Acta **5**, 369 (1932); L. D. Landau and E. M. Lifshitz, *Quantum Mechanics,* 3rd ed. (Pergamon, New York, 1979), pp. 347ff.

[19]An alternative procedure could apply if the value of $g'(\pi/2)$ were negligible. In that event the scale of ϕ could be anchored at $\theta=\pi/2$ by setting $\phi(\pi/2)=0$ and $y(\theta)$ would then coincide with $h^{1/2}Y_b^e(\phi)$ or $h^{1/2}Y_b^o(\phi)$.

[20]H. A. Bethe and E. E. Salpeter, *Quantum Mechanics of One- and Two-Electron Atoms,* (Springer-Verlag, Berlin, 1957), Sec. III.

[21]F. Herman and S. Skillman, *Atomic Structure Calculations* (Prentice-Hall, Englewood Cliffs, 1963).

[22]D. A. Harmin, Phys. Rev. A **24**, 2491 (1981).